International Conference on Applied Energy 2020
Dec. 1 - Dec. 10, 2020, Bangkok / Virtual
Paper ID: 0565

Multi-objective optimal sizing of a biomass fuelled hybrid Stirling engine coupled with an ORC decentralised micro-CCHP system

Godfrey T. Udeh[1,2*], Stavros Michailos[2], Derek Ingham[2], Kevin J. Hughes[2], Lin Ma[2], Mohamed Pourkashanian[2]

1. *Department of Mechanical Engineering, Faculty of Engineering, University of Port Harcourt, Nigeria.*
2. *Energy 2050, Department of Mechanical Engineering, University of Sheffield, Sheffield, S3 7RD, United Kingdom.*

ABSTRACT

The design optimisation of a hybrid Stirling-organic Rankine cycle driven micro-CCHP utilising biomass fuel and exhaust waste heat to produce power, cooling and heating is presented. Four objectives have been formulated from thermodynamic and economic points of view to optimise the design of the system including the energy utilisation efficiency, exergy efficiency, primary energy savings and artificial thermal efficiency of the system. While the cooling ratio and frequency of the Stirling engine prime mover have been selected as the decision variables. The non-dominated sorting genetic algorithm II (NSGA-II) has been deployed to solve the optimisation problem and produce a Pareto frontier of the optimal solutions. Further, using the TOPSIS approach, the optimal design parameters have been selected from the Pareto set. The study constitutes the first attempt to holistically optimise such a hybrid micro-CCHP in a robust manner. The results of the study optimise the design of the proposed system and this design will be used as basis, in the future, to carry out a dynamic simulation of a scaled-up case study.

Under optimal conditions, the design parameters are found to be frequency and cooling ratio of 29.11 Hz and 0.238, respectively and the performance indicators; energy utilisation efficiency, exergy efficiency, primary energy savings and artificial thermal efficiency are 0.85, 0.57, 0.51 and 0.62, respectively. The optimum SE-ORC based micro-CCHP system will produce 3.2 times more heating than cooling.

Keywords: Biomass fuel, Micro-CCHP, Optimisation, TOPSIS, Hybrid prime mover.

1. INTRODUCTION

External combustion engines such as the Stirling engines (SE) that utilise multiple clean fuels are promising prime movers for standalone micro-combined cooling, heating and power (CCHP) systems designed to cogenerate cooling, heating and electricity. In a recent study, it was found that using a hybrid SE and organic Rankine cycle (ORC) as the prime mover in micro-CCHP improved the performance of the standalone SE significantly [1].

For a system with several components and producing many energy vectors, the configuration of the system and speed of operation of the prime mover are key design parameters that affects its performance. To obtain the best configuration and optimal operating regime, a combination of multi-objective optimisation and multi-criteria decision making (MCDM) tools have been deployed. The optimisation of renewable decentralised systems is of paramount importance as this will result in more efficient designs and will eventually assist to phase out existing fossil fuel technologies.

Some previous studies have been conducted to optimise the design of the SE and ORC prime movers from single and multi-objective perspectives [2–7], but none of these studies consider the integration of SE with ORC. Several other studies focused on the multi-objective optimisation of different configurations of micro-CCHPs that utilise a variety of prime movers in a standalone or hybrid power mode from thermodynamic, economic and environmental viewpoints [8–11].

To the best of authors' knowledge, multi-objective optimisation from a thermoeconomic viewpoint has not been performed for a micro-CCHP fired by a hybrid of SE-ORC and this forms the basis for this study. First, a four-

Selection and peer-review under responsibility of the scientific committee of the 12th Int. Conf. on Applied Energy (ICAE2020).

objective optimisation is performed using a non-dominated sorting genetic algorithm which would present the optimal results in the form of a Pareto set. Subsequently, a MCDM tool is deployed to select the optimal design parameters from the Pareto set. This robust approach optimises the performance of the system and sets the foundation for further research on scaled-up cases.

2. SYSTEM DESCRIPTION AND FORMULATION OF THE OPTIMISATION MODEL OF THE MICRO-CCHP

Several micro-CCHP configurations have been deployed to meet the cooling, heating and electricity load demands of the end users. The configuration selected is determined by the energy vectors that are desired to be met (CCHP) as well as the energy resources available (wood chips) at the design location, i.e. remote regions in Nigeria.

In Fig 1, we present the proposed micro-CCHP concept that hybridises the SE and ORC to produce electricity, in a combined power configuration where the exhaust of the SE is utilised by the ORC. The flue gas produced after the combustion of the fuel, supplies the input energy is needed to produce power in the SE. Further, cooling is produced in the thermal chiller by utilising the recirculated waste flue gas to heat up its generator. Finally, waste heat discharged by the absorber and condenser of the thermal chiller is absorbed by the utility, and subsequently, it is boiled by the low grade recirculated flue gas to produce domestic hot water.

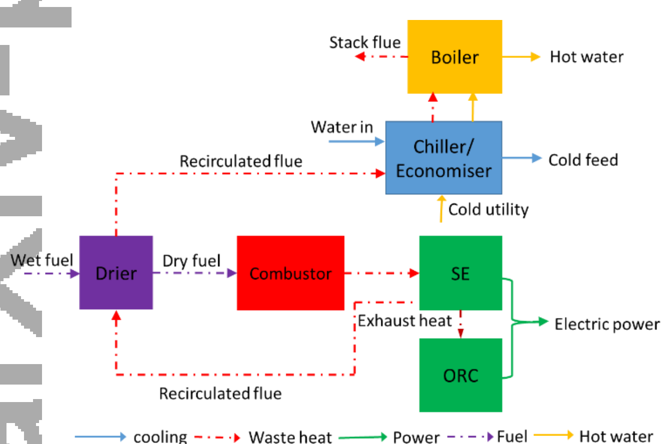

Fig. 1. Schematic diagram of the hybrid prime mover micro-CCHP.

The power output and thermal efficiency of the SE prime mover is obtained as follows [12]:

$$\dot{W}_{\mathrm{SE,actual}} = \left\{\left\{\oint (p_{\mathrm{e}} dV_{\mathrm{e}} + p_{\mathrm{c}} dV_{\mathrm{c}})\right\} - W_{\mathrm{FST}\ \&\ mech\ fric} - W_{\mathrm{pdrop}}\right\} Freq - \dot{W}_{\mathrm{Hyst}} \quad (1)$$

$$\eta_{\mathrm{SE}} = \frac{\dot{W}_{\mathrm{SE,actual}}}{\dot{Q}_{\mathrm{actual,h}}} \quad (2)$$

where, in Eq. (1), $W_{\mathrm{FST}\ \&\ mech\ fric}$ (J) is the combined loss from the engine due to finite speed and mechanical friction, W_{pdrop} (J) is the loss due to pressure drop in the engine and $\dot{W}_{\mathrm{Hyst}}$ (W) is the spring hysteresis loss, $Freq$ (Hz) is the frequency of the engine.

The actual heat added to the engine, $\dot{Q}_{\mathrm{actual,h}}$ is given by:

$$\dot{Q}_{\mathrm{actual,h}} = \dot{Q}_{\mathrm{quasi-ideal,h}} - \dot{Q}_{\mathrm{cond}} + \dot{Q}_{\mathrm{r,non-ideal}} - \dot{Q}_{\mathrm{leak}} - \dot{Q}_{\mathrm{diss,total}} \quad (3)$$

where $\dot{Q}_{\mathrm{quasi-ideal,h}}$ (W) is the heat gained in the heater in a quasi-ideal process, $\dot{Q}_{\mathrm{cond}}$ (W) is the conduction heat loss, $\dot{Q}_{\mathrm{r,non-ideal}}$ (W) is the heat lost due to the imperfection of the regenerator, $\dot{Q}_{\mathrm{leak}}$ (W) is the heat lost to leakage from the engine, and $\dot{Q}_{\mathrm{diss,total}}$ (W) is the heat lost due to energy dissipation as a result of the friction in the engine. Please refer to [12] for the comprehensive model of the SE used in this study.

The solution of the differential equations of the SE was implemented numerically in MATLAB while custom blocks in Aspen Plus® were used to model the performance of the other components.

2.1 *Multi-objective model formulation*

In this study, four performance metrics were selected as the objective functions based on the simulated data presented in Ref. [1]. The selected metrics for the multi-objective optimisation are: the energy utilisation factor (EUF_{CCHP}), exergy efficiency ($\eta_{II,CCHP}$), primary energy savings (PES_{CCHP}) and artificial thermal efficiency (ATE_{CCHP}) while the cooling ratio (cr) and frequency ($Freq$) of the prime mover are the dependent variables.

The optimization problem is presented as:

$$maximise\ \ f(X) = f_1(X), f_2(X), f_3(X), f_4(X) \quad (4)$$

$$X \epsilon \{X_1, X_2\} \quad (5)$$

Subject to:

$$X_{min} \leq X \leq X_{max} \quad (6)$$

Eq. (4) expresses the objective functions where f_1 is the EUF_{CCHP} $(-)$, f_2 is the $\eta_{II,CCHP}$ $(-)$, f_3 is the PES_{CCHP} $(-)$, and f_4 is the ATE_{CCHP} $(-)$ while the decision variables $X_1 \equiv Freq$ (Hz) and $X_2 \equiv cr$ $(-)$ are expressed in Eq. (5).

In Eq. (6), the constraints for the optimisation problem are presented showing the upper and lower bounds of the decision variables. The range of values used here are $Freq = [25, 58.33]$ and $cr = [0, 1]$.

2.1.1 Objective 1 (EUF_{CCHP})

$$EUF_{CCHP} = \frac{\dot{W}_{CCHP} + \dot{Q}_k + \dot{Q}_h}{\dot{m}_{\text{woodchips}} HHV} \tag{7}$$

where $\dot{W}_{CCHP} = \dot{W}_{SE,actual} + \dot{W}_{ORC}$ (W) is the combined electric power produced by the SE and ORC, $\dot{Q}_k$ (W) is the cooling load of the thermal chiller, $\dot{Q}_h$ (W) is the heat consumed by the boiler, $\dot{m}_{\text{woodchips}}$ (kg/s) is the feed rate of the biomass fuel and HHV (J/kg) is the heating value of the biomass on a dry basis.

2.1.2 Objective 2 ($\eta_{II,CCHP}$)

$$\eta_{II,CCHP} = \frac{\dot{W}_{CCHP} - \left(1 - \frac{T_0}{T_k}\right)\dot{Q}_k + \left(1 - \frac{T_0}{T_k}\right)\dot{Q}_h}{\left(1 - \frac{T_0}{T_{flue}}\right)\dot{Q}_{\text{CCHP}}} \tag{8}$$

where T_0 (K) is the dead state temperature, T_k (K) is the cooling temperature, T_h (K) is the heating temperature, and T_{flue} (K) is the temperature of the flue.

2.1.3 Objective 3 (PES_{CCHP})

$$PES_{CCHP} = 1 - \frac{\dot{Q}_{\text{CCHP}}}{\frac{\dot{W}_{CCHP}}{\eta_{elect,ref}} + \frac{\dot{Q}_h}{\eta_{h,ref}} + \frac{\dot{Q}_k}{\eta_{h,ref}\xi_{ref}}} \tag{9}$$

where $\dot{Q}_{\text{CCHP}}$ (W) is the total heat input into the CCHP, $\eta_{elect,ref}$ $(-)$ is the electrical efficiency of the reference plant, $\eta_{h,ref}$ $(-)$ is the electrical efficiency of a conventional boiler, ξ_{ref} $(-)$ is the reference

2.1.4 Objective 4 (ATE_{CCHP})

$$ATE_{CCHP} = \frac{\dot{W}_{\text{CCHP}}}{\dot{Q}_{CCHP} - \frac{\dot{Q}_h}{\eta_{h,ref}} - \frac{\dot{Q}_k}{\eta_{h,ref}\xi_{ref}}} \tag{10}$$

2.2 Optimisation method

In this paper, the non-dominated sorting genetic algorithm II (NSGA-II) was used to obtain the optimum solution in the form of a Pareto frontier. The NSGA-II optimisation algorithm has been implemented in MATLAB while an integration between MATLAB and Aspen plus® has been created to determine the objective functions by establishing a link that exchanges the necessary variables between the two software [1]. A population size of 50, generations of 100, cross over function intermediate, cross over fraction of 0.8 and Pareto fraction of 0.5 were set for the optimisation.

2.3 Decision making process

To select the best option out of the Pareto set, the technique for order preference by similarity to the ideal solution (TOPSIS) has been used in this study. The following are the steps in the TOPSIS decision making process:

i. Compute the weighted normalised optimised results. The weighted normalised data u_{ij} is given as:

$$u_{ij} = w_j.\frac{x_{ij}}{\sqrt{\sum_{i=1}^{n} x_{ij}^2}} \quad i = 1,2..n; j = 1,2..m \tag{11}$$

where w_j is the weight obtained from the decision matrix and x_{ij} are the optimised results.

ii. Calculate the separation of each of the weighted normalised results from the positive and negative ideal solutions, PIS and NIS, respectively. The Euclidean distance between an alternative and the PIS is given as:

$$D_i^+ = \sqrt{\sum_{j=1}^{n}\left(u_{ij} - u_j^+\right)^2} \, i = 1,2,\dots n \tag{12}$$

In a similar manner, the distance between an alternative and the NIS is given as:

$$D_i^- = \sqrt{\sum_{j=1}^{n}\left(u_{ij} - u_j^-\right)^2} \, i = 1,2,\dots n \tag{13}$$

where the positive ideal solution is $u_j^+ = \max_{\forall i} u_{ij}$ and the negative ideal solution is $u_j^- = \min_{\forall i} u_{ij}$.

iii. Calculate the ranking index and arrange the ranking indices in a descending order. The ranking index is given as:

$$RI_i = \frac{D_i^-}{D_i^- + D_i^+} \quad i = 1,2 \dots..n \tag{14}$$

The alternative with the highest RI_i is selected based on this approach.

The decision matrix and the criteria used to obtain the weight for each of the alternatives in this study is presented in Tables 1 and 2, respectively.

Table 1. Decision matrix from experts for TOPSIS analysis.

	EUF	η_{II}	PES	ATE
EUF	1	$1/4$	$1/3$	2
η_{II}	4	1	$1/2$	5
PES	3	2	1	3
ATE	$1/2$	$1/5$	$1/3$	1

Table 2. Judgement criteria for the decision matrix [13].

Intensity of importance	Definition
1	Equal importance
3	Weak importance
5	Essential or strong importance
7	Demonstrated importance
9	Absolute importance
2,4,6	Intermediate values

3. RESULTS AND DISCUSSION

The models for predicting the performance of the subsystems of the micro-CCHP have been validated against experimental data in Ref. [1] and very good agreements between the predicted results and experimental data have been observed. The models, developed in this study [1], have been used to obtain the objective functions and to implement the multi-objective optimisation. Here, the Pareto optimal frontier obtained from this multi-objective optimisation problem is presented both qualitatively and quantitatively.

Fig. 2 shows quantitatively the Pareto frontier of the optimal solutions in a 3-D plot when wood chips fuel containing 10 % moisture after drying is utilised to fire the micro-CCHP system. The conflict in these objectives is evidenced by the spread in the optimised data. As seen in Fig. 2, the optimal data present both dominated and non-dominated solutions. It is also evident that there is no single solution that maximises all the objectives; hence, the need to apply the TOPSIS MCDM tool to select the best alternative.

Based on the decision matrix presented in Table 1, the weight assigned to each of the objective functions are 12.68%, 36.07%, 42.57%, and 8.67%, for the EUF_{CCHP}, $\eta_{II,CCHP}$, PES_{CCHP} and ATE_{CCHP}, respectively. Using these weights and the steps described in Section 2.3, the TOPSIS scheme was deployed and the best option was selected. The TOPSIS best gave $EUF_{CCHP} = 0.85$, $\eta_{II,CCHP} = 0.57$, $PES_{CCHP} = 0.51$ and $ATE_{CCHP} = 0.62$. These values were obtained for the decision variables; $Freq = 29.11$ (Hz) and $cr = 0.238$ $(-)$. Thus, at the optimum design conditions, the designed micro-CCHP will operate at low to medium speed and produce at least 3 times more heating than cooling.

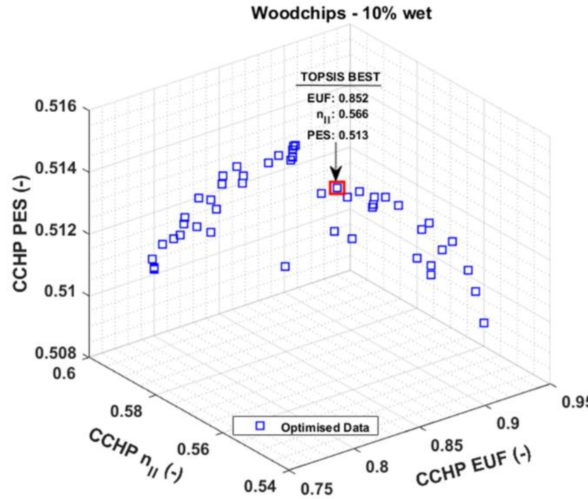

Fig. 2. Pareto frontier of the optimised result and the TOPSIS best solution.

In the qualitative presentation shown in Fig. 3 – 6, the Pareto optimal frontier has been plotted on the simulated data for each of the objective functions against the decision variables. The TOPSIS best selected for each of the objective functions is also indicated in these figures. In Fig. 3 and 4, the scatter in the optimal results were mainly localised around the region with low frequency and low cooling ratio. However, high scatter distribution is seen in Fig. 5 and 6 for the EUF_{CCHP} and the ATE_{CCHP} which also presented more variation in the simulated data.

Although the $\eta_{II,CCHP}$ and PES_{CCHP} (Fig. 3 and 4) indicated global optima at the medium/high frequency and low cooling ratio region, the Pareto optimal frontier was localised within the low frequency region. This is because the EUF_{CCHP} and ATE_{CCHP} (Fig. 5 and 6) indicated global optima in this domain, which then buttresses the conflicting nature of the multi-objective problem.

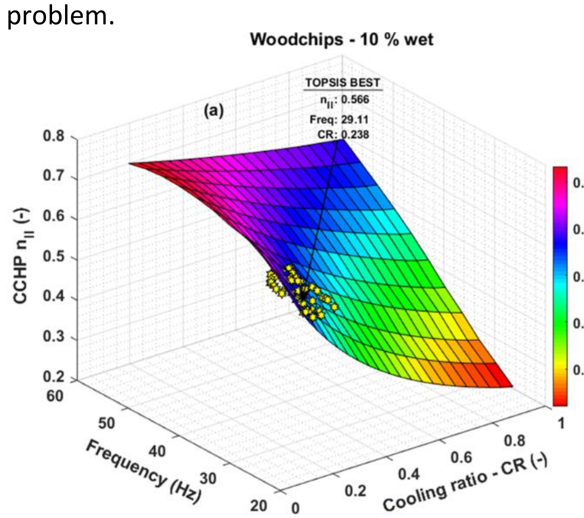

Fig. 3. Optimised exergy efficiency plotted against the decision variables and showing the TOPSIS best.

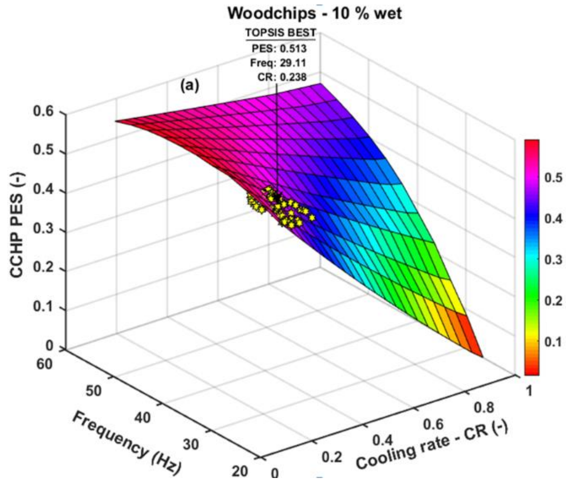

Fig. 4. Optimised results of the PES plotted on the initial simulated data showing the TOPSIS best.

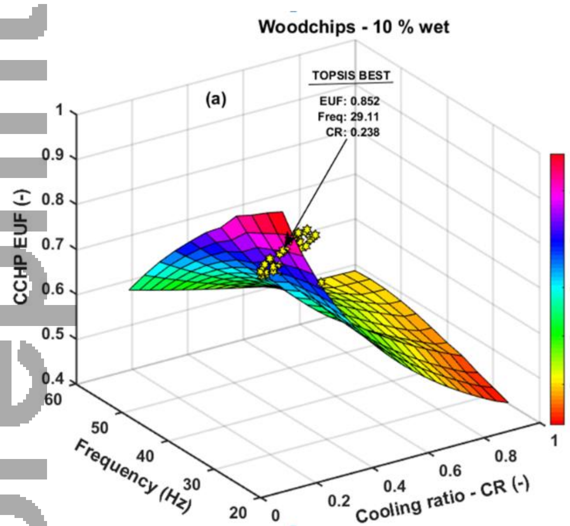

Fig. 5. Optimised EUF plotted on the initial simulated data and showing the TOPSIS best.

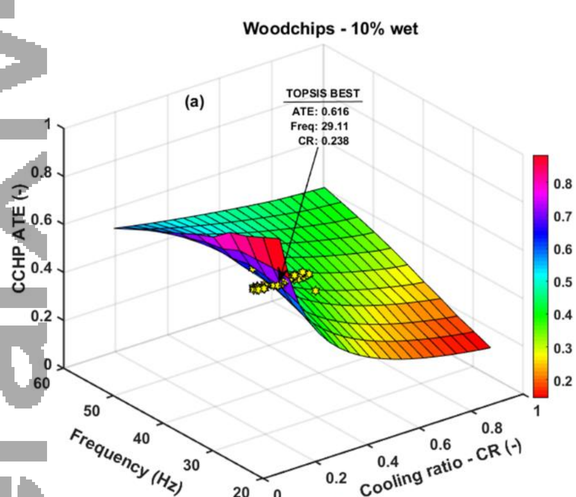

Fig. 6. Optimsed ATE results plotted on the simulated data showing the TOPSIS best.

4. CONCLUSIONS

Based on the maximisation of EUF_{CCHP}, $\eta_{II,CCHP}$, PES_{CCHP} and ATE_{CCHP}, multi-objective sizing optimisation of a novel micro-CCHP configuration has been undertaken. A combination of the NSGA-II multi-objective optimisation algorithm and the TOPSIS decision making tool were deployed to solve the optimisation problem and select the best configuration. From the obtained Pareto optimal solution set, an alternative has been selected. The selected alternative ensured a trade-off in the objectives and produced EUF_{CCHP}, $\eta_{II,CCHP}$, PES_{CCHP} and ATE_{CCHP} of 0.85, 0.57, 0.51 and 0.62, respectively. The optimal design parameters of the system support the prime mover to operate at low speed and the system to have a generating capacity of heating and cooling loads in the ratio of 76.2% to 23.8%. The optimised design will be used to investigate the techno-economic feasibility of scaled-up cases and further integration with solar/wind applications to enhance reliability.

ACKNOWLEDGEMENT

This study was funded by the Petroleum Technology Development Fund, an agency of the Ministry of Petroleum Resources, in Nigeria.

REFERENCE

[1] Udeh GT, Michailos S, Ingham D, Hughes KJ, Ma L, Pourkashanian M. A techno-enviro-economic assessment of a biomass fuelled micro-CCHP driven by a hybrid Stirling and ORC engine. Energy Convers Manag 2021;227:113601. doi:10.1016/j.enconman.2020.113601.

[2] Patel V, Savsani V, Mudgal A. Many-objective thermodynamic optimization of Stirling heat engine. Energy 2017;125:629–42. doi:10.1016/j.energy.2017.02.151.

[3] Toghyani S, Kasaeian A, Hashemabadi SH, Salimi M. Multi-objective optimization of GPU3 Stirling engine using third order analysis. Energy Convers Manag 2014;87:521–9. doi:10.1016/j.enconman.2014.06.066.

[4] Zhao C, Zheng S, Zhang J, Zhang Y. Exergy and economic analysis of organic Rankine cycle hybrid system utilizing biogas and solar energy in rural area of China. Int J Green Energy 2017;14:1221–9. doi:10.1080/15435075.2017.1382362.

[5] Yang F, Zhang H, Song S, Bei C, Wang H, Wang E. Thermoeconomic multi-objective optimization of an organic Rankine cycle for exhaust waste heat recovery of a diesel engine. Energy 2015;93:2208–28. doi:10.1016/j.energy.2015.10.117.

[6] Cheng CH, Yang HS. Optimization of geometrical parameters for Stirling engines based on theoretical

analysis. Appl Energy 2012;92:395–405. doi:10.1016/j.apenergy.2011.11.046.
[7] Xiao G, Sultan U, Ni M, Peng H, Zhou X, Wang S, et al. Design optimization with computational fluid dynamic analysis of β-type Stirling engine. Appl Therm Eng 2017;113:87–102. doi:10.1016/j.applthermaleng.2016.10.063.
[8] Izadiamoli N, Sayyaadi H. Conceptual design, optimization, and assessment of a hybrid Otto-Stirling engine/cooler for recovering the thermal energy of the exhaust gasses for automotive applications. Energy Convers Manag 2018;171:1063–82. doi:10.1016/j.enconman.2018.06.056.
[9] Entezari A, Manizadeh A, Ahmadi R. Energetical, exergetical and economical optimization analysis of combined power generation system of gas turbine and Stirling engine. Energy Convers Manag 2018;159:189–203. doi:10.1016/j.enconman.2018.01.012.
[10] Hosseinpour J, Sadeghi M, Chitsaz A, Ranjbar F, Rosen MA. Exergy assessment and optimization of a cogeneration system based on a solid oxide fuel cell integrated with a Stirling engine. Energy Convers Manag 2017;143:448–58. doi:10.1016/j.enconman.2017.04.021.
[11] Sadeghi M, Chitsaz A, Mahmoudi SMS, Rosen MA. Thermoeconomic optimization using an evolutionary algorithm of a trigeneration system driven by a solid oxide fuel cell. Energy 2015;89:191–204. doi:10.1016/j.energy.2015.07.067.
[12] Udeh GT, Michailos S, Ingham D, Hughes KJ, Ma L, Pourkashanian M. A new non-ideal second order thermal model with additional loss effects for simulating beta Stirling engines. Energy Convers Manag 2020;206. doi:10.1016/j.enconman.2020.112493.
[13] Saaty TL. A scaling method for priorities in hierarchical structures. J Math Psychol 1977;15:234–81. doi:10.1016/0022-2496(77)90033-5.